



Orbital Debris

Quarterly News

Volume 28, Issue 4
October 2024

Inside...

NASA's ODPO Wins Software of the Year Award 2

Aerodynamic Demise Model for Carbon Fiber Polymer Fiber 3

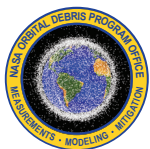
DebrisSat: 10 years and Growing 5

Meeting Reports 8

Upcoming Meetings 9

NASA ODPO Abstracts 10

Space Missions and Satellite Box Score 11



A publication of the NASA Orbital Debris Program Office (ODPO)

Three New On-orbit Fragmentations

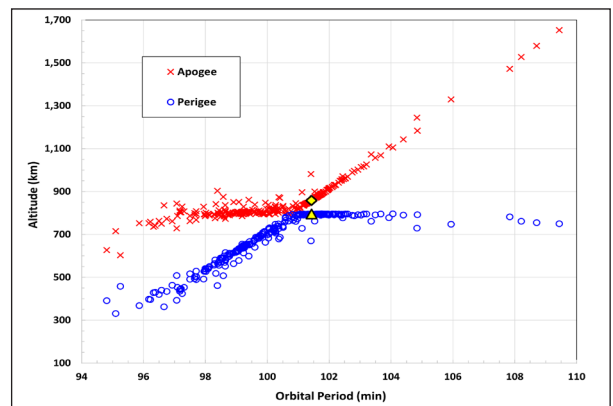
The 18th Space Defense Squadron (18 SDS) of the U.S. Space Force identified three on-orbit fragmentation events during the past quarter. The first breakup was associated with the Russian Resurs P1 spacecraft (International Designator 2013-030A, U.S. Satellite Catalog Number 39186). The 6-metric-ton, remote-sensing spacecraft was launched in 2013 and decommissioned in 2022. The breakup occurred at 16:32 GMT on 26 June 2024. The orbit of Resurs P1 at the time of the breakup was approximately 388 km × 353 km, with an inclination of 97 degrees. Due to the low altitude of the Resurs P1 orbit, many fragments reentered shortly after the event before being cataloged. As of 26 August 2024, 18 fragments have been added to the U.S. Satellite Catalog and 17 of them have reentered.

The second breakup was associated with the Defense Meteorological Satellite Program (DMSP) 5D-2 F8 spacecraft (International Designator 1987-053A, U.S. Satellite Catalog Number 18123) at 20:41 GMT on 19 July 2024. The orbit of DMSP 5D-2 F8 at the time of the breakup was approximately 837 km × 818 km, with an inclination of 98.7 degrees. The 700-kg spacecraft was launched in 1987 and decommissioned in 2006. Four fragments associated with the event were identified by the 18 SDS and added to the U.S. Satellite Catalog as of the end of July. DMSP 5D-2 F8 is one of the “Block 5D-2 Family” of spacecraft, similar in design to other Block 5D-2 and Block 5D-3 families of DMSP and NOAA spacecraft. DMSP 5D-2 F11, DMSP 5D-2 F13, NOAA-16 (5D-3), and NOAA-17 (5D-3) experienced

major breakups between 2004 and 2021, and the root cause of those events was likely battery related (ODQN vol. 25, issue 4, December 2021, pp. 5-7).

The third breakup was associated with a Long March 6A (CZ-6A) upper stage after its successful deployment of the first 18 spacecraft for China’s *Qianfan* large constellation. The 18 SDS detected the breakup of this CZ-6A upper stage (International Designator 2024-140U, U.S. Satellite Catalog Number 60397), which had a dry mass of approximately 5800 kg, at 17:15 GMT on 6 August 2024. The orbit of 2024-140U was close to 857 km × 797 km, with an inclination of 89 degrees. As of 15 September 2024, 283 large fragments have been cataloged.

continued on page 2



The Gabbard diagram of the 2024-140U CZ-6A fragments, based on their cataloged elements dated 15 September 2024. The apogee and perigee altitudes of the parent CZ-6A upper stage are also shown as yellow diamond and yellow triangle, respectively.

On-orbit Fragmentations

continued from page 1

The Gabbard diagram shows that most of them are concentrated between 500 km and 900 km altitudes. Prior to this breakup, another CZ-6A upper stage, 2022-151B, also experienced a major breakup at 847 km x 813 km in 2022 (ODQN vol. 27, issue 1, March 2023, pp. 1-2). To date, 793 large fragments from the breakup of 2022-151B have been cataloged, making it the fourth worst historical breakup event and the number one worst

breakup of an upper stage in history. It is likely that hundreds of thousands of fragments too small to be tracked but large enough to threaten missions were also generated from the breakups of the two CZ-6A upper stages. Due to their relatively high orbits, the CZ-6A fragments will have non-trivial, long-term negative effects to the environment and to spacecraft operating in the vicinity for years to come. ♦

NASA's Orbital Debris Program Office Wins Software of the Year Award



The NASA's Orbital Debris Program Office's (ODPO) Orbital Debris Engineering Model (ORDEM) was awarded the NASA Software of the Year. ORDEM is the agency's primary tool for modeling and mitigating the risk of orbital debris collisions with spacecraft, which is critical to mission safety and success.

ORDEM provides a timely, validated model of the human-made orbital debris environment. It facilitates modeling assessments by spacecraft owners and operators, as well as ground-based observation planning.

The NASA ODPO began development of ORDEM in the mid-1980s in support of the Space Station Program Office. The first computer-based version of ORDEM was released in 1996 as ORDEM96 and pioneered the use of debris population ensembles characterized by altitude, eccentricity, inclination, and size. ORDEM2000 replaced the curve-fitting approach with a finite element representation of the debris environment. ORDEM 3.0 represented a significant upgrade in terms of model features and capabilities. It extended the model to the

geosynchronous orbit region (up to 40,000 km), which enabled analysis of more varied orbits – such as geosynchronous transfer orbits and other highly elliptical spacecraft orbits – and sensor orientations. Additional upgrades included an expansion of observation program datasets in underrepresented regions and the addition of uncertainties on the reported orbital debris flux. Most significantly, ORDEM 3.0 included a distribution in material density of orbital debris fluxes.

ORDEM 3.1 was created to include the same capabilities as ORDEM 3.0 and incorporate updated datasets available to NASA for both constructing and validating the modeled orbital debris populations. On 15 November 2021, the Russian Federation tested a direct-ascent anti-satellite weapon on their Cosmos 1408 spacecraft. The resulting large cloud of debris was of sufficient size and concern that the ODPO created an update of the ORDEM model (ORDEM 3.2) to include the effects of this new cloud.

ORDEM is the second most requested software from Johnson Space Center and is also available via a web application accessible at <https://ordem.appdat.jsc.nasa.gov/>.

Dr. Mark Matney, modeling lead for the ODPO, accepted the award on behalf of the team during the ASCEND Conference. Additional details on the award can be found here: <https://www.nasa.gov/organizations/otps/2024-software-of-the-year-cowinner-orbital-debris-engineering-model-ordem/>. ♦

Subscribe to the ODQN or Update Your Subscription Information

To be notified by email when a new issue of the ODQN is placed online, or to update your personal information, please navigate to the ODQN subscription page on the NASA Orbital Debris Program Office (ODPO) website at: <https://orbitaldebris.jsc.nasa.gov/quarterly-news/subscription.cfm>. The ODPO respects your privacy. Your email address will be used solely for communication from the ODQN Managing Editor.

PROJECT REVIEW

Aerodynamic Demise Model for Carbon Fiber Reinforced Polymer

B. GREENE

The Object Reentry Survival Analysis Tool (ORSAT) is the primary NASA computer code used to assess reentry survivability of spacecraft. This survivability prediction is required to determine the risk to humans on the ground, in accordance with NASA-STD 8719.14. The most recent release, version 7.1, includes a more complex, strength-based, material demise model for carbon fiber reinforced polymers (CFRP). ORSAT version 7.0 introduced a pyrolysis model for CFRP and glass fiber reinforced polymer (GFRP) mass loss but only considered complete demise of the material through phase change (sublimation or melting) of the remaining fibers and char matrix. While the silica fibers in GFRP melt at around 1200 K (a temperature often reached in reentry environments), sublimation of the graphite fibers in CFRP at the relevant pressure range starts to occur at around 3000 K, more than twice the typical temperatures encountered in low Earth orbit reentry. Without another demise mechanism, complete demise of CFRP is nearly impossible.

The new aerodynamic demise model calculates the point in the trajectory where the resin matrix has charred enough and the aerodynamic forces have become large enough to begin ripping the component into small clumps of carbon fiber chaff. At each time step, the maximum bending stress in the component is calculated based on the shape, size, and layup thickness, and the current ultimate stress of the material is calculated based on the amount of pyrolyzed resin. When the bending stress exceeds the ultimate stress, the component is considered to have demised.

The strength reduction is modeled using empirical fits to laboratory test data collected by the NASA Orbital Debris Program Office (ODPO) in the University of Texas at Austin's inductively coupled plasma (ICP) torch facility and the Johnson Space Center Experimental Impact Laboratory. Samples of epoxy-, vinyl ester-, and phenolic-based CFRP materials and an epoxy-based GFRP material were exposed to a range of heat flux values in the ICP torch between 15 W/cm² and 30 W/cm² for durations ranging from 5 seconds to 30 seconds. The ultimate strength of each coupon was then determined using a Chatillon TCD1000 tensile test machine configured with a three-point bending jig. A more detailed description of the test procedure and results can be found in [1]. Ultimately, for ORSAT's built-in generic carbon fiber/epoxy and glass fiber/epoxy materials, the exponential relationships between mass loss and ultimate strength and the logarithmic relationships between char depth and ultimate strength, shown in Figure 1, were chosen. The ultimate strength at 0% mass loss is set at each material's average ultimate strength, and the models are capped at this value. Even though the built-in strength models for CFRP and GFRP can depend on either mass loss or char depth, the ORSAT subroutine for calculating a material's ultimate strength additionally supports correlations with peak temperature, adding flexibility in the definition of user-supplied material properties.

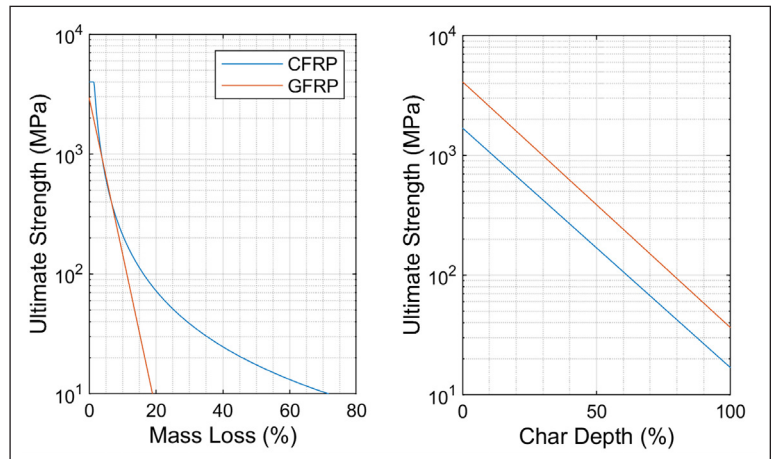


Figure 1. Plots of ultimate strength models for CFRP and GFRP based on mass loss (left) and char depth (right).

Calculating the maximum bending stress within the component requires two main simplifying assumptions:

- The component's shape is reasonably approximated by one of the six primitive solids that ORSAT supports: sphere, cylinder, cone, disk, plate, or box.
- The component comprises only a thin shell of carbon fiber with no significant stiffening members and no other layers of materials.

The first assumption is very often true of CFRP and GFRP parts on spacecraft, as these parts tend to take the form of things like bipod legs, rectangular structural panels, circuit boards, spherical and cylindrical pressure vessels, or box enclosures. The second assumption precludes several types of spacecraft components such as carbon overwrapped pressure vessels (COPVs) and CFRP face sheet/aluminum honeycomb sandwich panels. Many observed space debris reentries, higher fidelity reentry simulation studies, and wind tunnel tests have shown that the majority of COPVs survive to the ground [2, 3, 4, 5]. Wind tunnel tests have also shown that face sheets on sandwich panels are quickly separated from the core material by the flow, at which point the CFRP component conforms to the simplifying assumptions [6].

The equations used for the stress within the CFRP shell are derived from plate theory in the cases of plates, disks, and boxes, and membrane theory in the cases of spheres, cylinders, and cones [7, 8]. The derivation of the stress equation for each shape starts with a free-body diagram of the forces and moments on a finite element of the surface. Figure 2 shows this diagram of the pressure, p_{dyn} , counteracted by the inertial force per unit area, apt , the normal forces, N_x and N_y , and the shear forces T_{xy} , T_{yx} , and T_z . The moments acting on the element are the bending moments M_{xy} and M_{yx} and the torsion moments M_x and M_y .

continued on page 4

Aerodynamic Demise Model

continued from page 3

Summing the forces and moments to zero sets up a system of differential equations. Depending on the shape of the component, different simplifying assumptions can be applied, and the forces on the finite element are integrated to find the stress distribution over the surface. The maximum stress is calculated by finding the roots of the derivative of the stress distribution and solving for the stress at those locations. This analysis results in the equations given in the Table, where r is the radius; t is the thickness of the shell or plate; p_{dyn} is the dynamic pressure at the stagnation point;

F_{drag} is the total drag force on the component; a is the acceleration of the component; ρ is the density of the material; B is a tabulated coefficient for stress in a simply supported flat plate; and l , w , and h are the length, width, and height, respectively.

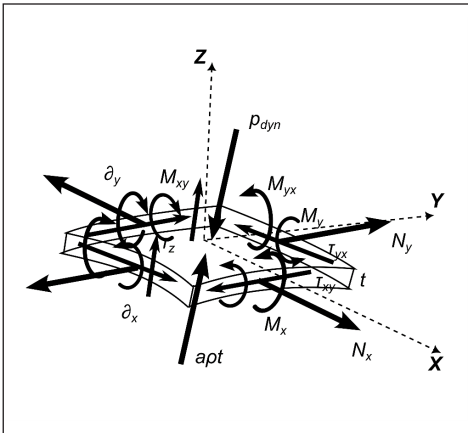


Figure 2. Free-body diagram of a surface stress element.

A sample ORSAT run for a CFRP plate of 3 different thicknesses released at 78 km altitude is shown in Figure 3. It shows the ultimate strength of the plate material begins to drop as it starts to pyrolyze and the bending stress in the plate increases rapidly. In the case of the thinnest plate, these two values quickly meet and the plate demises. The medium thickness plate also demises, but the pyrolysis process takes longer than the thinner plate and the maximum stress is lower. The thickest plate survives to the ground as it neither fully pyrolyzed, nor reached a maximum stress great enough to break. If the aerodynamic shredding model is not invoked all three plates survive to the ground with varying amounts of mass loss. For the thinnest plate, this is unrealistic as the maximum temperature far exceeds the value needed to fully pyrolyze the resin matrix, leaving the fibers with no cohesion at all.

With the FRP aerodynamic demise model, ORSAT can predict the reentry demise of many common CFRP and GFRP spacecraft components with much less conservatism and provide spacecraft operators with a more realistic projection of a spacecraft's reentry human casualty risk. Further improvements to the aerodynamic demise model are currently under development, including expanding the model to non-pyrolyzing materials and incorporating more of the standard ORSAT primitive shapes. A model for oxidative ablation of graphite fibers and other high-temperature materials is also under development to further refine the material demise models in ORSAT.

continued on page 5

Table. Maximum stress equations for supported shapes in ORSAT 7.1.

Shape	Maximum Stress
Sphere	$\frac{p_{dyn}}{2t}(r + r^3)$
Cylinder	$\frac{F_{drag}}{2\pi r t}(\frac{6}{t} + 1)$
Cylinder (end-on)	$\frac{0.696 p_{dyn} r^2}{t^2}$
Box	$B(l, w) p_{dyn} \frac{h^2}{t^2}$
Flat Plate	$\frac{3lw}{2h} \left(-\frac{\rho h}{4} + \frac{95}{384} p_{dyn} \right)$
Disk	$\frac{6}{t^2} \left((p_{dyn} + \rho t) \left(\frac{945}{64} - 15r^2 \right) + \frac{16r}{7} - \frac{12}{7r} \right)$

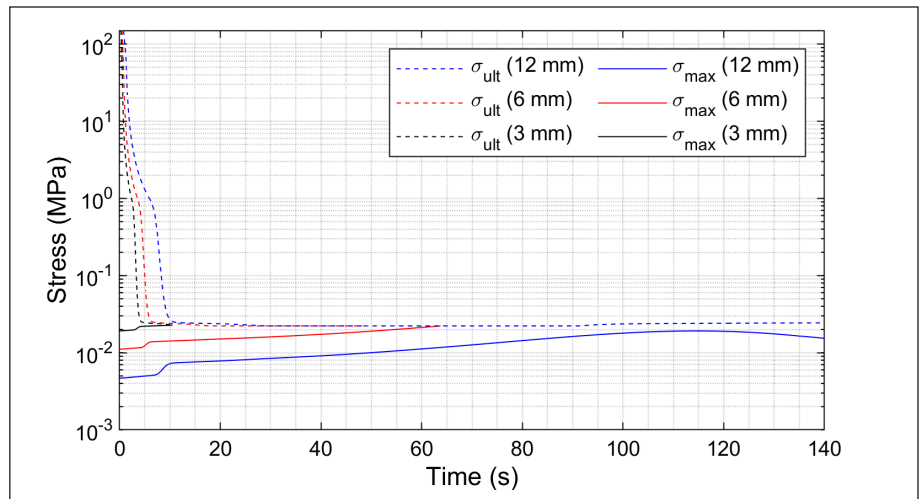


Figure 3. Plot of maximum stress and ultimate stress for three simulated flat plates of CFRP in ORSAT with length of 0.8 m, width of 0.58 m, and thickness of 3 mm, 6 mm, and 12 mm.

Aerodynamic Demise Model

continued from page 4

References

1. Mendoza, P., Greene, B., and Ostrom, C., Aerodynamic Demise Model Implementation to Object Reentry. In *2nd International Orbital Debris Conference*, Sugar Land, TX, (2023).
2. Roulette, J. "SpaceX Rocket Debris Lands on Man's Farm in Washington", *The Verge*, Apr 2, 2021, <https://www.theverge.com/2021/4/2/22364582/spacex-rocket-debris-falls-farm-washington> Accessed August 4, 2024.
3. Molczan, T., "Re-entry Sightings and Debris Recovery of 2008-010B Spain-2015 November 03 UTC," *Journal of Space Safety Engineering*, vol. 2 issue 2, pp. 83-90, (2015).
4. Lips, T., *et al.* "About the Demisability of Propellant Tanks During Atmospheric Re-Entry from LEO." In *8th International Space Safety Conference*, Melbourne, FL, (May 2016).
5. El Rassi, J., *et al.*, "Plasma testing of miniaturized Composite Overwrapped Pressure Vessels in reentry conditions," In *Aerospace Europe Joint 10th EUCASS-9th CEAS Conference*, Switzerland, July 9-13, 2023.
6. Annaloro, J., *et al.*, Rebuilding with PAMPERO of destructive hypersonic tests on honeycomb sandwich panels in the T-117 wind tunnel. *Journal of Space Safety Engineering*, vol. 7, issue 2, pp. 113-124, (2020).
7. Kelly, P. *Solid Mechanics part II: Engineering Solid Mechanics Small Strain*. Section 6, pp. 120-187 The University of Auckland, (2013).
8. Truesdell, C. The Membrane Theory of Shells of Revolution. *Transactions of the American Mathematical Society*, vol. 58, pp. 96-166, (1945). ♦

DebrisSat: 10 Years and Growing

H. COWARDIN, J. OPIELA, J.-C. LIOU, A. KING, AND J. MELO

In 2014, a series of hypervelocity impact tests were conducted at the U.S. Air Force Arnold Engineering Development Complex (AEDC) in support of updating satellite breakup models used by NASA and the Department of Defense (DOD), details presented in the Table. The DebrisSat project is a collaboration between the NASA Orbital Debris Program Office (ODPO); the Space Force Space Systems Command (SSC), formerly the Air Force Space and Missile Systems Center; The Aerospace Corporation; and the University of Florida (UF). The team worked to design and build a representative low Earth orbit spacecraft that was constructed with modern techniques and materials. To ensure a successful test, AEDC procedures called for a range check pretest and a full "dress rehearsal" test before the main shot. The NASA Hypervelocity Impact Technology (HVIT) team provided the

optional pretest target: a multi-shock shield impacted using the same projectile and planned velocities that would be used for DebrisSat [1].

Following the successful pre-test, DebrisLV ("launch vehicle") was constructed by The Aerospace Corporation as a lower-fidelity target for the dress rehearsal test using shot parameters similar to the HVIT pretest. Also included in the DebrisLV test were three-density polyurethane foam stacks to verify that the build of the soft-catch material lining walls of the tank would be sufficient for a successful DebrisSat impact test. This second shot also provided technical benefits to studying breakup events of a scaled-down launch vehicle upper stage composed primarily of metal components. The DebrisLV was a success, but the impact highlighted the need for additional soft-catch foam build-up behind the target to mitigate a blowout downrange.

continued on page 6

Table. Test parameters for the HVIT pre-test, DebrisLV, and DebrisSat test campaigns.

	HVIT pre-test	DebrisLV	DebrisSat
Target body dimensions	2.6 m (length) multi-shock shield	35 cm (dia) × 88 cm (ht)	60 cm (dia) × 50 cm (ht)
Target mass	56 kg* <i>multi-shock blankets only</i>	17.1 kg	56 kg
Projectile material	Hollow Al cylinder with attached nylon bore-rider	Hollow Al cylinder with attached nylon bore-rider	Hollow Al cylinder with attached nylon bore-rider
Projectile dimensions/mass	8.6 cm × 9 cm, 598 g	8.6 cm × 9 cm, 598 g	8.6 cm × 9 cm, 570 g
Impact speed	6.9 km/sec	6.9 km/sec	6.8 km/sec
Impact Energy to Target Mass ratio (EMR)	14.2 MJ	14.2 MJ	13.2 MJ
Soft-Catch System: Polyurethane foam stacks	None	3 densities: 0.048, 0.096, and 0.192 g/cm ³ ; ≤ 51 cm thick	3 densities: 0.048, 0.096, and 0.192 g/cm ³ ; ≤ 61 cm thick

DebrisSat

continued from page 5

After recovering all the fragments from this test, cleaning up the entire chamber, and packaging the soft-catch foam and loose materials for shipment, the DebrisSat test was successfully conducted on 15 April 2014. The test chamber was again emptied and cleaned, the foam and debris were boxed, and the materials

from the DebrisLV and DebrisSat tests were shipped to UF for characterization. Using the NASA Standard Satellite Breakup Model (SSBM), the original estimate for the total number of fragments of size 2 mm and larger that would be generated was calculated to be approximately 85,000. The team at UF continues

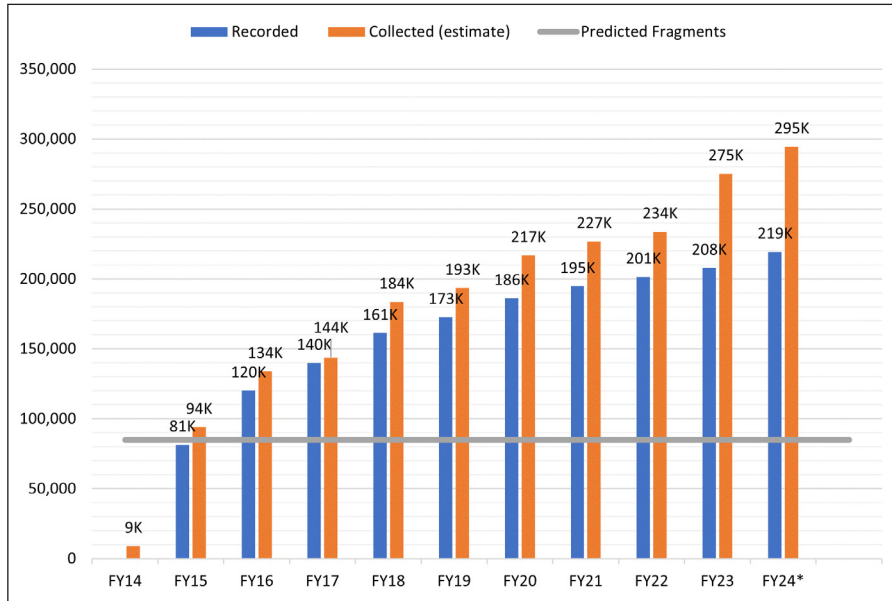


Figure 1. Recorded and collected fragments for each FY since impact test. "Predicted Fragments" denotes the predicted number with characteristic length ≥ 2 mm. "Recorded" fragments represent data that has been uploaded into the database and "Collected" include all fragments visually assessed to have a dimension approximately 2 mm and larger. (*Data through 4 September 2024).

to work toward characterizing the over 294,000 fragments collected, which will be used to support updates to the NASA SSBM in addition to providing a rich dataset to update the optical size estimation model (SEM) and radar SEM (ODQN vol. 28, issue 3, pp. 3-5).

After the successful design, fabrication, and impact test, the DebrisSat project continues to focus on meeting two data recovery goals that will be used to improve space situational awareness applications and satellite breakup models for better orbital debris environment definition: 1) collect and characterize all fragments down to 2 mm in size and 2) recover 90% (50.4 kg) of the original mass (56.0 kg). Figures 1 and 2 show the status for recovered fragments approximately ≥ 2 mm and the recovered mass, respectively, as of 4 September 2024. Note that one of the DebrisSat project's goals is to recover and characterize all objects 2 mm and larger in characteristic length, defined as the average of the three greatest, orthogonal, projected dimensions. Since triage of the fragments takes place before calculation of characteristic length, fragments are usually selected by their longest physical dimension, which results in some characterized fragments with characteristic length less than 2 mm. The collection of fragments began shortly after the impact test, with an estimated total of 9000 fragments collected (*i.e.*, isolated and packaged) that same U.S. Government Fiscal Year (FY). One year later, the recorded (*i.e.*, entered in to the DebrisSat database) and estimated collected counts surpassed the SSBM estimates for fragments ≥ 2 mm. Ten years later, the estimated number of collected fragments is nearly 3.5 times higher than original model estimates. The recovered mass to date is 46.42 kg, or 92.1%, of the goal.

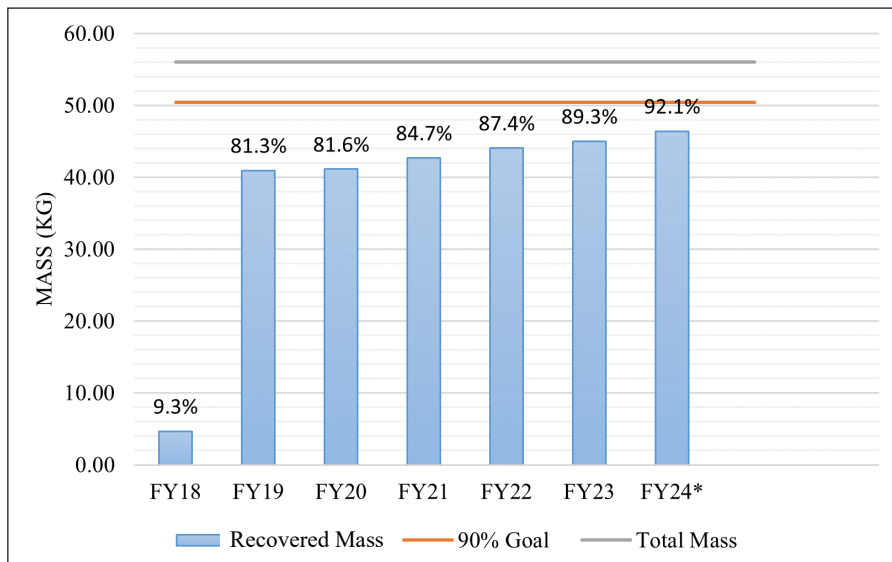


Figure 2. Collected mass from FY18-24 as a percentage of goal. (*Data through 4 September 2024).

Much of the discrepancy between the predicted and measured counts is a result of the use of carbon fiber reinforced polymer (CFRP), which is used in many modern spacecraft for structural support as well as in composite-wrapped pressure vessels. This material constitutes the majority of fragments with sizes below 12 mm in characteristic length (Lc) as

continued on page 7

DebrisSat

continued from page 6

shown in Figure 3. The characteristic length is used as the size parameter, being the average of the object's three maximum orthogonal projected dimensions, and the SSBM line in Figure 3 is scaled to the mass collected to date. By fragment primary material classification, other dominant materials include (in decreasing abundance for the < 10 mm populations): metal (a general classification that includes known aluminum, stainless steel, and titanium as well as fragments that have not yet been resolved into one of those categories via density verification and ongoing work applying machine learning), copper (Cu – primarily wires), plastic, and epoxy.

Another important aspect is the shape parameterization. Understanding the shape distributions of fragments generated by breakup events is key to improving the fidelity of orbital debris impact risk assessments; thus, it is one of the primary drivers leading the next major update of the NASA Orbital Debris Engineering Model (ORDEM). The HVIT team, in coordination with NASA Johnson Space Center's White Sands Test Facility, has been working to test non-spherical projectiles and run simulations to characterize the effects from cylindrical and plate-like projectiles of various materials impacting standard shield configurations based on the results from the DebrisSat test (ODQN vol. 28, issue 3, pp. 3-5). The current shape distributions based on the recorded DebrisSat data are shown in Figure 4. CFRP tends to break into plate- and rod-like fragments, whereas the metals are mostly associated with nuggets, parallelepipeds, and spheroids. The flexible category encompasses materials that do not retain their shapes (*i.e.*, wires or multi-layered insulation).

The DebrisSat project benefits from the lessons learned from previous impact tests, such as the 1992 Satellite Orbital Debris Characterization Impact Test (SOCIT). These two major impact tests provide vast amounts of information – laboratory corollaries for on-orbit breakup events from 1960s-era spacecraft to current designs used in low Earth orbit. The DebrisSat team has moved away from manual size estimates via calipers, implementing a series of imagers for 2D and 3D measurement of fragments, with data stored in a database for easy query [2]. Additionally, the team at UF has started to use machine learning in two research areas: 1) to assist in properly assigning complex

fragments to density bins and 2) for X-ray image processing of foam panels to automatically determine fragment size, shape, density, and location without needing to extract the fragments [3, 4]. In addition to the lessons learned in performing and measuring the results of such a large-scale test, DebrisSat has

continued on page 8

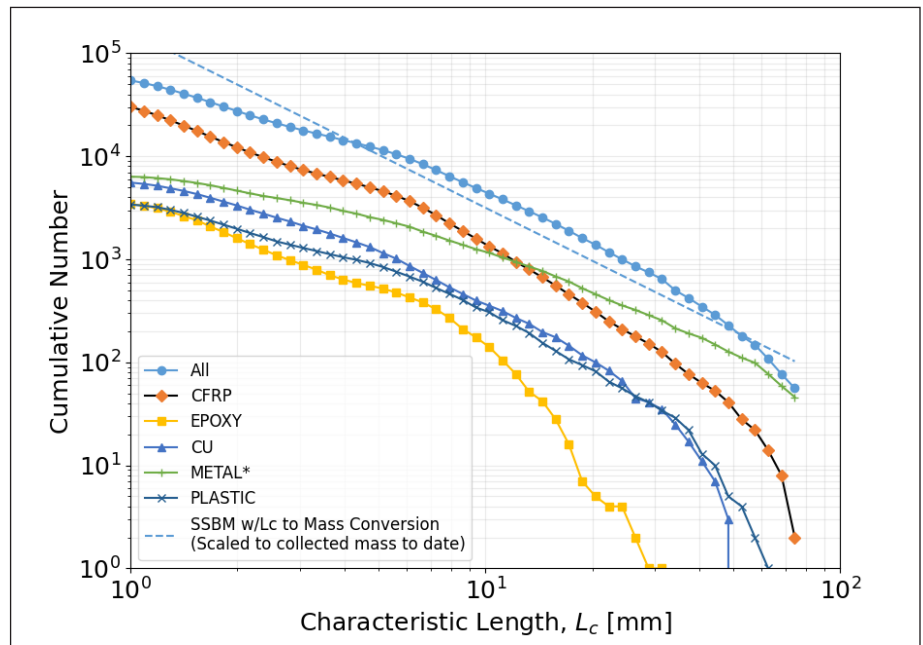


Figure 3. Cumulative number of fragments as function of size (L_c) for most prominent materials.

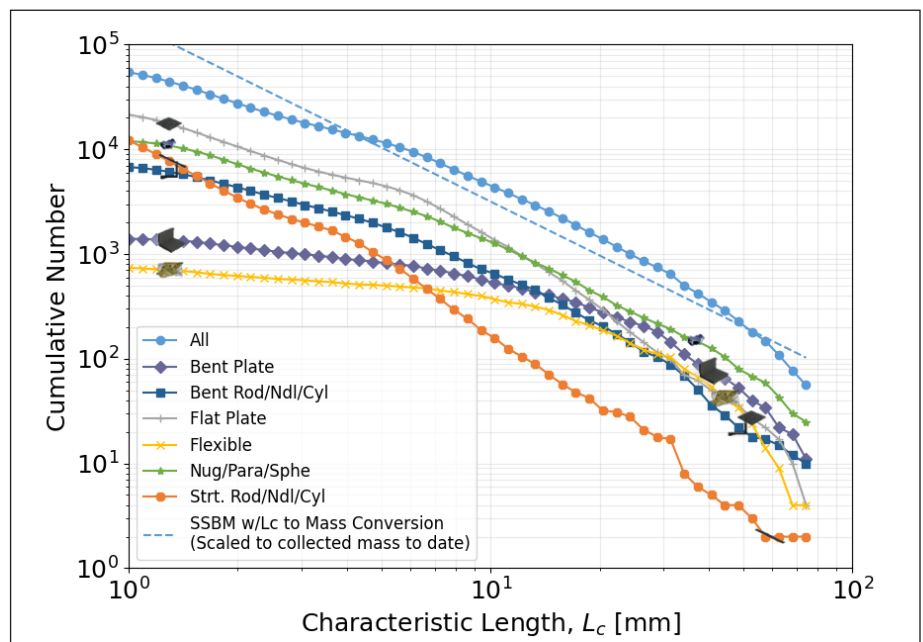


Figure 4. Cumulative number of fragments as function of size (L_c) for shape categories.

DebrisSat

continued from page 7

provided a wealth of data that will be used in various efforts to update engineering and environmental models for NASA and the DOD for years to come.

References

1. Miller, J., *et al.*, “Multi-Shock Shield Performance At 14 MJ for Catalogued Debris,” *Procedia Engineering*, Vol 103, pp 405-412, 2015.
2. Toledo, R., Shiotani, B., and Fitz-Coy, N., “Imaging Systems Utilized in the DebrisSat Fragment Size,” *IOC 2019*, December 2019.
3. Ondes, B., *et al.*, “NASA DebrisSat – Verification of Material Characterization Processes by Utilization of Machine Learning Algorithms,” *IOC 2023*, December 2023.
4. Siam, S. A., *et al.*, “Using Machine Learning to Infer Material Properties of Debris Fragments from X-ray Images in the DebrisSat Project,” *IOC 2023*, December 2023. ♦

MEETING REPORTS

10-11 June 2024: 7th Space Debris Modeling and Remediation Workshop, Toulouse, France

The 7th Space Debris Modeling and Remediation Workshop, hosted by the French space agency *Centre National d’Études Spatiales* in Toulouse, France, 10-11 June 2024, brought together international experts to discuss the growing challenges posed by space debris and ongoing efforts to mitigate them. Presentations and discussions covered a wide range of topics, including talks on modeling for sustainability and mitigation as well as remediation solutions and techniques. Additional topics can be found in the high-level agenda: <https://iaaspace.org/wp-content/uploads/iaa/Scientific%20Activity/debrisminutes03246.pdf>.

Some of the highlights were discussions on calls for action for strengthening regulations, active debris removal (ADR) development, improved modeling, and international cooperation. The workshop emphasized the urgency of a concerted effort to combine international mitigation efforts, technological development, and cooperation to ensure a sustainable space environment for future generations. ♦

24-26 June 2024: 2024 Trilateral Safety and Mission Assurance Conference (TRISMAC) Frascati, Rome, Italy

The European Space Agency (ESA) hosted the 2024 Trilateral Safety and Mission Assurance Conference (TRISMAC) at its European Space Research Institute (ESRIN) in Frascati (Rome), Italy, on 24-26 June. Approximately 100 international subject matter experts attended the conference, most representing the safety and mission assurance (SMA) organizations at ESA, Japan Aerospace Exploration Agency, and NASA.

The theme of this year’s TRISMAC is “Space Exploration: New Challenges and Opportunities. New space, new players, and new destinations: challenges and opportunities for SMA.” The conference covered six topics from the unique SMA

perspective: lunar exploration; digital engineering and assurance; sustainability; lessons learned and return of experience; assurance of new technologies; and new partners and acquisition. The three-day event consisted of keynotes, including one by former NASA astronaut Rex Walheim discussing a Commercial LEO Space Station and another address by former ESA astronaut Frank De Winne entitled “An Astronaut Perspective to Safety and Mission Assurance”. There were also technical presentations on various SMA topics, such as orbital debris, planetary protection, and nuclear flight safety. Additional details on the meeting can be found at <https://nikal.eventsair.com/trismac-2024/>. ♦

13-21 July 2024: 45th Committee on Space Research (COSPAR) Scientific Assembly, Busan, South Korea

The 45th Committee on Space Research (COSPAR) Assembly was held in Busan, South Korea, from 13-21 July 2024 at the Busan Exhibition and Convention Center (BEXCO). More than 60 countries were represented by over 2600 participants, with 365 posters exhibited and more than 2300 presentations given. The conference consisted of daily panel sessions and plenary presentations and offered 147 parallel scientific tracks.

The eight-day conference covered a broad range of topics related to space, from modeling atmospheres; tracking and characterizing asteroids; developing spacecraft for planetary exploration; and orbital debris. The panel on Potentially Environmentally Detrimental

Activities in Space (PEDAS) orbital debris sessions covered three full days, including 39 oral presentations and two workshop sessions, one on debris mitigation compliance software and another on optical observations of orbital debris. ODPO gave an invited talk highlighting NASA’s activities in orbital debris entitled “The NASA Orbital Debris Program Office – In Service of Space Safety.” The orbital debris sessions highlighted continued improvements in measuring and modeling the orbital debris environment as well as potential solutions in mitigating and remediating debris.

More information can be found at <https://cospar2024.org/>. ♦

Meeting Reports

continued from page 8

19 August 2024: The NASA-DOD Orbital Debris Working Group Meeting, Colorado Springs, Colorado, USA

The 27th annual NASA-DOD Orbital Debris Working Group (ODWG) was held in Colorado Springs, Colorado, on 19 August 2024. This annual one-day meeting provides the framework for cooperation and collaboration between NASA-DOD on orbital debris-related activities, such as measurements, modeling, mitigation, and policy development. NASA and the DOD have benefited significantly from this meeting, and many collaborations directly result from this WG. The meeting was co-chaired by the NASA Orbital Debris Program Office (ODPO) and by the Operational Assessments Division, HQ Space Operations Command, United States Space Force (USSF).

The USSF and the NASA ODPO provided opening remarks, followed by a series of presentations from members representing NASA and DOD. The ODPO opened with a presentation on recent the Haystack Ultrawideband Satellite Imaging Radar, Goldstone Radar, and the Eugene Stansbery-Meter Class Autonomous Telescope optical observations of the orbital debris environment. The ODPO then provided an update on the development of the ODPO's *in situ* debris sensor, the Multi-layer Acoustic & Conductive-grid Sensor and its upcoming flight demonstration mission. Additionally, the ODPO presented the status of the

Orbital Debris Engineering Model (ORDEM) 4.0 development and other modeling activities. This presentation was followed by an update on the DebrisSat project and the fusion of measurements and analysis from the project into the next generation ORDEM 4.0 and NASA Standard Satellite Breakup Model. The final ODPO presentation included updates on reentry and orbital safety activities, including the recent release of Debris Assessment Software 3.2.6 and the inspection of a recovered fragment of the Dragon 2 Trunk that reentered over Australia in July 2022.

DOD personnel presented an overview of the radar cross-section calculation process followed by the 18th Space Defense Squadron (18SDS) at Vandenberg Space Force Base and a discussion of recent on-orbit breakups (ODQN vol. 28, issue 4, pg. 1). The succeeding DOD presentation concerned efforts in space domain awareness and methods to track and catalog spacecraft in cislunar space. The final DOD presentation consisted of updates on the Space Fence on Kwajalein Atoll, the Space Surveillance Telescope in Western Australia, and an overall status of the Space Surveillance Network, including the transitions to the Alpha-5 and nine-digit, two-line element (TLE) numbering schemes. ♦

UPCOMING MEETINGS

1-4 April 2025: 9th European Conference on Space Debris, Bonn, Germany

The 9th European Conference on Space Debris, hosted by the European Space Agency, will be held at the World Conference Center in Bonn, Germany. The conference provides a forum to discuss different aspects of space debris research, including measurements, environmental models, risk analysis techniques, protection designs, mitigation and remediation, and policy and regulation. Abstract submissions open 1 October 2024 and close 15 November 2024. Additional details on the conference are available at: <https://space-debris-conference.sdo.esoc.esa.int/>. ♦

NASA Orbital Debris Photo Gallery

The NASA Orbital Debris Photo Gallery has high resolution, computer-generated images of objects in Earth orbit that are currently being tracked. Photos and graphics may be freely downloaded from the NASA Orbital Debris Program Office webpages, unless they include a third-party credit line. In these cases, permission must be granted by the copyright owner. The Photo Gallery link is: <https://orbitaldebris.jsc.nasa.gov/photo-gallery/>.

ABSTRACTS FROM THE NASA ORBITAL DEBRIS PROGRAM OFFICE

The 25th Advanced Maui Optical and Space Surveillance Technologies Conference (AMOS),
17-20 September 2024, Maui, Hawaii

Analysis of Darkened Fragments Resulting from Laboratory Hypervelocity Experiments

HEATHER COWARDIN, PHILLIP ANZ-MEADOR, CORBIN CRUZ, JOHN OPIELA, JAROD MELO, MARK CASTANEDA, ERIC CHRISTIANSEN, CHRIS CLINE

NASA's Orbital Debris Program Office (ODPO) relies on measurements from optical, radar, and *in situ* measurements to facilitate the development of data-driven orbital debris environmental engineering models such as the NASA Orbital Debris Engineering Model (ORDEM). For optical measurements, the ODPO relies on ground-based optical telescopes to statistically assess objects in geosynchronous orbit (GEO) and, in the future, low Earth orbit (LEO). The data collected include the detected object's orbital parameters, time of observation, and optical magnitude. The latter parameter can be converted to a size using NASA's optical Size Estimation Model (oSEM). It is well known that the observed magnitude of orbital debris can vary based on an object's material constituents, observational geometry, and the effects of space weathering.

To assess these magnitude variations, the ODPO uses the Optical Measurement Center at NASA Johnson Space Center to characterize a variety of materials and fragments from laboratory impact tests representative of fragments that constitute the orbital debris population. One experiment was DebrisSat: a 56 kg spacecraft was built to incorporate structural elements of a modern LEO spacecraft and was subjected to a hypervelocity impact test at the U.S. Air Force's Arnold Engineering Development Complex using test parameters that may be encountered in LEO. The DebrisSat project has provided an abundance of information for assessing fragmentation debris in terms of material, color, shape, size, density, mass, and other derived parameters. Prior to the impact test, the ODPO collected spectral measurements on a subset of the materials

used to construct DebrisSat for a "ground-truth" of their optical properties. After the successful hypervelocity impact test, the DebrisSat team observed a fine, dark dust coating all the fragments. Prior research has suggested that this came from ablated material deposited on the fragments during the impact test, causing a change in the reflective properties [1]. Given that this lower reflectivity on the DebrisSat fragments will influence the laboratory-acquired magnitudes used to calculate size and inform potential updates to the oSEM, it is critical to assess if this darkening effect on the DebrisSat fragments is a laboratory bias or something that could occur in on-orbit breakup events.

This paper will provide a brief overview of the OMC and DebrisSat experiment, focused on the optical characterization of a subset of materials using broadband photometric measurements and spectroscopic measurements. In addition, elemental analysis of various DebrisSat fragments and the soft-catch foam used in the hypervelocity experiment compared with pristine foam will be examined to further evaluate the source of the dark material coating all fragments. Finally, the authors will present a twofold plan 1) for assessing potential biases in laboratory impact experiments that could affect laboratory optical characterization and 2) mitigating biases when compared with ground-based optical telescopic measurements of the orbital debris environment.

References

1. Radhakrishnan, G., *et al*, "Debris Characterization, Albedo, and Plume Measurements from Laser Ablations of Satellite Materials in High-Vacuum and in Gaseous Ambients," Proceedings of the 2018 AMOS Conference, Maui, Hawaii, September 2018. ♦

Announcements

The ODPO has an opening for a postdoctoral fellow via the [NASA Postdoctoral Program](#). This position would support an *in situ* sensor in development to characterize the small (millimeter-sized) orbital debris environment in low Earth orbit. Opportunities are available to support the development of the sensor and provide oversight and analyses that directly support future flight missions. For more information on this position, please see the [request](#).

Abstracts

The 7th International Workshop on Debris Modeling and Remediation, 10-11 June 2024, Toulouse, France A Survey of Modeling Activities by NASA’s Orbital Debris Program Office

MARK MATNEY

NASA’s Orbital Debris Program Office (ODPO) develops and maintains a number of modeling tools to analyze and simulate the orbital debris environment. One of the most important products produced by the NASA ODPO is the Orbital Debris Engineering Model (ORDEM). This model can be used by satellite designers and operators to design missions for better protection against the debris environment. The ODPO is currently working on the next generation, designated ORDEM 4.0. ORDEM 4.0 will include many known features from previous models, such as the ability to input a spacecraft orbit and time and the ability to compute the flux as a function of debris size, impact speed, impact direction, and debris material densities, as well as uncertainty information on the flux. A new addition will be a parameterized debris shape model based on laboratory hypervelocity impact tests, including DebrisSat. ORDEM is primarily based on dedicated debris measurements, such as by the Haystack Ultrawideband Satellite Imaging Radar (HUSIR), NASA’s Goldstone radar, and

observations of geosynchronous orbits (GEO) using the Eugene Stansbery-Meter Class Autonomous Telescope (ES-MCAT).

In addition to ORDEM, the ODPO also maintains other models, such as the LEO-to-GEO Environment Debris (LEGEND) model for studies of long-term evolution of Earth’s debris environment, with the ability to study various mitigation and remediation strategies. Another model, the Satellite Breakup Risk Assessment Model (SBRAM), is used to analyze how satellite breakups may affect critical space missions (such as the ISS) on short notice.

In addition to these models, the ODPO maintains other secondary models used to model satellite explosions and collisions, analyze radar, optical, and *in situ* data, and to model such things as solar activity and orbit evolution.

In this presentation, a survey of these models will be presented, showing how the different models are used together to create a comprehensive picture of Earth’s debris environment.



The 45th Committee on Space Research (COSPAR) Scientific Assembly, 13-21 July 2024, Busan, Korea The NASA Orbital Debris Program Office - In Service of Space Safety

CHRIS OSTROM

Since the NASA Orbital Debris Program Office’s (ODPO) founding in 1979 at the Johnson Space Center in Houston, Texas, it has been at the forefront of orbital debris research, modeling, and policy development. The ODPO has worked in collaboration with NASA and other U.S. government missions since the 1980s to mitigate the growth of the orbital debris environment and protect the population of the Earth.

Two main products from the ODPO, the Orbital Debris Engineering Model (ORDEM) and the Debris Assessment Software (DAS), are frequently among the top three most-downloaded software packages from the NASA Software Catalog. These products are provided free of charge to the public in furtherance of the goal to ensure that new space missions, in compliance with NASA’s orbital debris mitigation requirements, are developed,

operated, and disposed of responsibly. In addition to these external-facing software tools, the ODPO maintains high-fidelity internal tools for reentry simulation (the Object Reentry Survival Analysis Tool, ORSAT), short-term risk assessment for robotic and human spaceflight missions (the Satellite Breakup Risk Assessment Model, SBRAM), among others.

Using data from the ORDEM model, as well as using the Meteoroid Environment Model (MEM) developed by the Meteoroid Environment Office (MEO) at NASA’s Marshall Space Flight Center, the Hypervelocity Impact Technology (HVIT) team uses the BUMPER code to assess penetration risk to space vehicles in Earth orbit and beyond. This paper will discuss the services that the ODPO and HVIT provide, from mission concept development through end-of-mission, for NASA-related and commercial missions.



INTERNATIONAL SPACE MISSIONS								
1 May 2024 – 31 July 2024								
Intl.* Designator	Spacecraft	Country/ Organization	Perigee Alt. (KM)	Apogee Alt. (KM)	Incl. (DEG)	Addnl. SC	Earth Orbital R/B	Other Cat. Debris
1998-067	ISS dispensed objects	Various	403	416	51.6	1	0	0
2024-081A	LEGION 1	US	512	519	97.6	0	0	0
2024-081B	LEGION 2	US	513	518	97.6			
2024-082A	STARLINK-31749	US	443	445	43.0	22	0	0
2024-083A	CHANG'E 6	PRC		LUNAR SURFACE		0	1	0
2024-083C	ICECUBE-Q	PAKI		LUNAR ORBIT				
2024-084A	STARLINK-31589	US	442	446	43.0	22	0	0
2024-085A	OBJECT A	PRC	474	489	97.4	0	0	0
2024-085B	OBJECT B	PRC	489	507	97.4			

continued on page 12

SATELLITE BOX SCORE

(as of 04 September 2024, cataloged by the U.S. SPACE SURVEILLANCE NETWORK)

Country/ Organization	Spacecraft*	Spent Rocket Bodies & Other Cataloged Debris	Total
CHINA	709	4482	5191
CIS	1563	5403	6966
ESA	97	27	124
FRANCE	96	534	630
INDIA	108	92	200
JAPAN	210	104	314
UK	697	1	698
USA	8342	4975	13317
OTHER	1139	79	1218
Total	12961	15697	28658


* active and defunct

Visit the NASA
Orbital Debris Program Office Website
<https://orbitaldebris.jsc.nasa.gov>

Technical Editor
Heather Cowardin, Ph.D.

Managing Editor
Ashley Johnson

Correspondence can be sent to:
Laura Sorto
laura.g.sorto@nasa.gov



National Aeronautics and Space Administration
Lyndon B. Johnson Space Center
2101 NASA Parkway
Houston, TX 77058
www.nasa.gov
<https://orbitaldebris.jsc.nasa.gov/>

INTERNATIONAL SPACE MISSIONS

1 May 2024 – 31 July 2024

continued from page 11

Intl.* Designator	Spacecraft	Country/ Organization	Perigee Alt. (KM)	Apogee Alt.(KM)	Incli. (DEG)	Addnl. SC	Earth Orbital R/B	Other Cat. Debris
2024-085C	OBJECT C	PRC	489	507	97.4			
2024-085D	OBJECT D	PRC	497	511	97.4			
2024-085E	OBJECT E	PRC	419	491	97.37			
2024-086A	STARLINK-32108	US	443	445	43.0	22	0	0
2024-087A	ZHIHUI TIANWANG-1 01A	PRC	20164	20200	53.2	0	1	0
2024-087B	ZHIHUI TIANWANG-1 01B	PRC	20166	20198	53.2			
2024-088A	STARLINK-11107	US	359	361	53.2	19	0	0
2024-089A	SHIYAN 23 (SY-23)	PRC	592	601	97.8	0	1	0
2024-090A	STARLINK-31472	US	443	445	43.0	22	0	0
2024-091A	STARLINK-11125	US	359	360	53.2	19	0	0
2024-092A	COSMOS 2576	CIS	444	451	97.2	9	0	0
2024-093A	STARLINK-31363	US	443	445	43.0	22	0	0
2024-094A	OBJECT A	PRC	493	495	97.5	3	0	0
2024-095A	OBJECT A	PRC	520	534	97.6	3	0	0
2024-096A	USA 354	US	312	318	70.0	20	0	0
2024-097A	STARLINK-31947	US	443	445	43.0	22	0	0
2024-098A	STARLINK-31654	US	442	446	43.0	22	0	0
2024-099A	PREFIRE-2	US	518	538	97.5	0	2	0
2024-100A	STARLINK-31974	US	443	445	43.0	22	0	0
2024-101A	EARTHCARE	ESA	396	400	97.0	0	0	0
2024-102A	TIANQI 25	PRC	891	906	45.0	3	0	0
2024-103A	PROGRESS MS-27	CIS	413	420	51.6	0	1	0
2024-104A	PAKSAT MM1R	PAKI	35786	35788	0.0	0	1	0
2024-105A	OBJECT A	PRC	526	548	98	4	0	0
2024-106A	STARLINK-31872	US	443	445	43.0	22	0	0
2024-107A	STARLINK-11145	US	339	341	53.2	19	0	0
2024-108A	PREFIRE-1	US	518	538	97.5	0	2	0
2024-109A	STARLINER CALYPSO 1	US	413	420	51.6	0	0	0
2024-110A	OBJECT A	PRC	534	553	97.6	2	1	0
2024-111A	STARLINK-31978	US	446	448	53.2	21	0	0
2024-112A	STARLINK-11129	US	339	341	53.2	19	0	0
2024-113A	STARLINK-11181	US	359	361	53.2	19	0	0
2024-114A	KINEIS-1B	FR	633	640	98.0	4	2	0
2024-115A	SES-24	SES	8571	66242	11.4	0	1	0
2024-116A	OBJECT A	PRC	625	632	29.0	0	1	
2024-116B	OBJECT B	PRC	626	634	29.0			
2024-117A	STARLINK-31441	US	457	459	53.2	21	0	0
2024-118A	STARLINK-11201	US	337	341	53.2	19	0	0
2024-119A	GOES-U	US	35772	35800	0	0	1	0
2024-120A	STARLINK-32043	US	447	448	53.2	22	0	0
2024-121A	USA 375	US	293	356	70.0	20	0	0
2024-122A	CHINASAT-3A	PRC	35777	35796	0.0	0	1	0
2024-123A	ALOS-4	JPN	630	632	97.9	0	0	0
2024-124A	STARLINK-11168	US	338	341	53.2	19	0	0
2024-125J	CATSAT	US	469	543	97.3	7	1	0
2024-126A	TIANHUI 5C	PRC	604	606	97.8	0	1	1
2024-126B	TIANHUI 5D	PRC	604	607	97.8			
2024-127A	TURKSAT 6A	TURK	35783	35792	0.1	0	1	0
2024-128B	3CAT-4	SPN	567	585	62.0	7	1	0
2024-129A	STARLINK-11214	US	134	140	53.3	1	0	0
2024-130A	OBJECT A	PRC	250	649	97.5	0	1	0
2024-131A	STARLINK-32138	US	382	384	53.2	22	0	0
2024-132A	STARLINK-32156	US	389	390	53.2	22	0	0
2024-133A	STARLINK-11147	US	340	340	53.2	20	0	0
2024-134A	USA 396	US	ELEMS. NOT AVAILABLE			2	1	0

Intl. = International; SC = Spacecraft; Alt. = Altitude; Incli. = Inclination; Addnl. = Additional; R/B = Rocket Bodies; Cat. = Cataloged
Notes: 1. **Orbital elements are as of data cut-off date 31 July.** 2. Additional spacecraft on a single launch may have different orbital elements. 3. Additional uncatalogued objects may be associated with a single launch.